

THE FORCE TRACKING CONTROL OF ELECTRO-HYDRAULIC SYSTEM BASED ON PARTICLE SWARM OPTIMIZATION

PISAN MOONUMCA AND NATTAWOOT DEPAIWA

Department of Mechanical Engineering
Faculty of Engineering
King Mongkut's Institute of Technology Ladkrabang
No. 1, Chalongkrung Rd., Ladkrabang, Bangkok 10520, Thailand
{ m_pisankmitl; depaiwa }@hotmail.com

Received November 2015; revised March 2016

ABSTRACT. *This paper presents the optimal gains of backstepping controller by using the particle swarm optimization technique. The mathematical model is developed by Newton's second law, compressible fluid flow and flow rates of valve. The control law is formulated by employing a Control Lyapunov Function. The core feature of this paper is the combination of the backstepping and particle swarm optimization for optimal performance of controller. The controller gains are determined in automatic selection gains by minimizing the integral of time multiplied by absolute error function on step input. The fitness value can be guaranteed to the convergence of controller gains. The implementations are separated into two cases which are the real and estimated state feedbacks. The experiment has illustrated to find optimal controller gains. The results are also compared with the tracking response of real and estimated state measures in step and square signal. The results show a better tracking performance by using the strong particle swarm optimization (PSO) algorithm.*

Keywords: Particle swarm optimization, Electro-hydraulic system, Optimal controller gains

1. Introduction. Hydraulic system may be the first choice for power transmission in heavy-duty applications due to its advantages such as high power-to-weight ratio, fast response, high stiffness and high load capability. Major parts of electro-hydraulic systems (EHS) include the power unit, oil pipeline, control valve and hydraulic actuators. Normally, the force of the hydraulic cylinder is controlled by varying the valve command [1] in order to control the flow rate in and out of the actuator. The nonlinearities appear in term of the relationship between the hydraulic flow rate and the cylinder pressure; hence, the relationship between the command input and cylinder force is nonlinear. The nonlinear behavior creates a challenge in the design of controller for electro-hydraulic systems.

Various linear control techniques were implemented to control EHS's in the past [2,3]. Classical linearization techniques based on the root mean square (RMS) error prediction were proposed and implemented [2]. The controller was implemented on single-input and single-output (SISO) plant that was decoupled from multiple-input and multiple-output (MIMO) system. The result with small steady state error was shown. A proportional-integral-derivative (PID) controller with feedback linearization was presented [3]. The control system was designed without the consideration of friction. Since many nonlinear behaviors need to be linearized in order to be controlled by linear controllers which may not be suitable. Some researchers used nonlinear controller to solve this problem. Several nonlinear controllers were also investigated [4-9]. Sliding mode with friction compensation [4] was proposed and high accuracy performance was achieved. However, when the

controller was implemented with friction compensation turned off, the tracking performance was less than satisfactory. Lyapunov algorithm based controller [5] was proven to be effective when the system has uncertainty parameters.

Backstepping is a popular nonlinear control methodology that is applied when designing most controllers for nonlinear systems such as hydraulic systems, flight control and chemical reactor systems. Its methodology has been developed continuously in order to achieve performance target. The designed backstepping control for a continuous-stirred tank reactors (CSTRs) is shown in [6]. The controller performances are compared with the standard PI controller. Backstepping controllers for position tracking of an EHS are modeled in [7]. The model simulation used a sinusoidal reference input on top of which disturbances of about 10% were applied to each state. The resulting controller predicted good tracking performance and robustness to disturbances. Backstepping controllers for electro-hydraulic systems were presented in [8] and [9]. Nonlinear adaptive robust motion control of electro-hydraulic servo systems was presented in [10]. The incorporation between backstepping and another technique was presented as artificial intelligent technique and optimization algorithm [11,12]. In [11] the backstepping parameters were tuned by neural network to improve the tracking performance of mobile robots. The backstepping controller tuned by fuzzy logic was implemented for stabilizing and attitude control of a quad-rotor helicopter [12]. Searching for optimal parameters of a backstepping controller is difficult such as trial and error. Moreover, the tuning process could be time-consuming and the target performance cannot be guaranteed. To solve the problems, the particle swarm optimization (PSO) algorithm is an alternative technique for tuning the backstepping controller. PSO was widely investigated in [13,14], and proved its ability to solve the optimization problems. The PSO is powerful for searching optimal variables for solving complex control problems [15] and it could be able to solve for optimal power flow of electric energy [16]. PSO has been applied to various controllers because of its faster convergence compared with other techniques such as Genetic Algorithm [17]. The optimization of backstepping control parameters is presented in [18] comparing two algorithms, namely PSO and gravitational search algorithm (GSA). The simulation results have shown that the backstepping controller with PSO outperformed the same controller with GSA technique. A significant requirement of backstepping design is full-state feedback which is, however, not always possible due to cost, space limitations and measurement noise. The estimated state based backstepping control that is used for the SISO nonlinear uncertain system is presented in [19]. However, the study was based on simulation results rather than experiments.

In this paper, the search for optimal parameters of a backstepping controller in a force tracking EHS is proposed. The PSO algorithm is used to tune for the optimum backstepping gain. The current investigation presents two experimental approaches: real measured states and using a reduced order state observer.

Nomenclature

A_1 = Piston area side head-end	P_t = Reservoir pressure
A_2 = Piston area side rod-end	u = Control signal
β = Effective bulk modulus	Q_1 = Flow rate of head-end side
c = Viscous coefficient	Q_2 = Flow rate of rod-end side
F_{spring} = Spring action force	V_1 = Volumes cylinder of head-end
K_v = Flow/signal gain of valve	V_2 = Volumes cylinder of rod-end
k_s = Stiffness of spring	V_{01} = Initial head-end volume
m = Mass of piston	V_{02} = Initial rod-end volume
P_1 = Pressure side head end	V_{in} = Command voltage

P_2 = Pressure side rod end x_p = Piston's displacement
 P_s = Supply pressure γ = Piston areas ratio (A_1/A_2)

2. System Description. Figure 1 shows the schematic diagram of the EHS used in this study. A linear spring is connected to the end of the piston rod and acts as a resistive load. The mathematical model for force control of the EHS is obtained using Newton's second law and compressible flow [20]. The force balance on the piston is shown in Equation (1), where friction is neglected for simplicity.

$$m\ddot{x}_p = P_1A_1 - P_2A_2 - c\dot{x}_p - F_{spring} \tag{1}$$

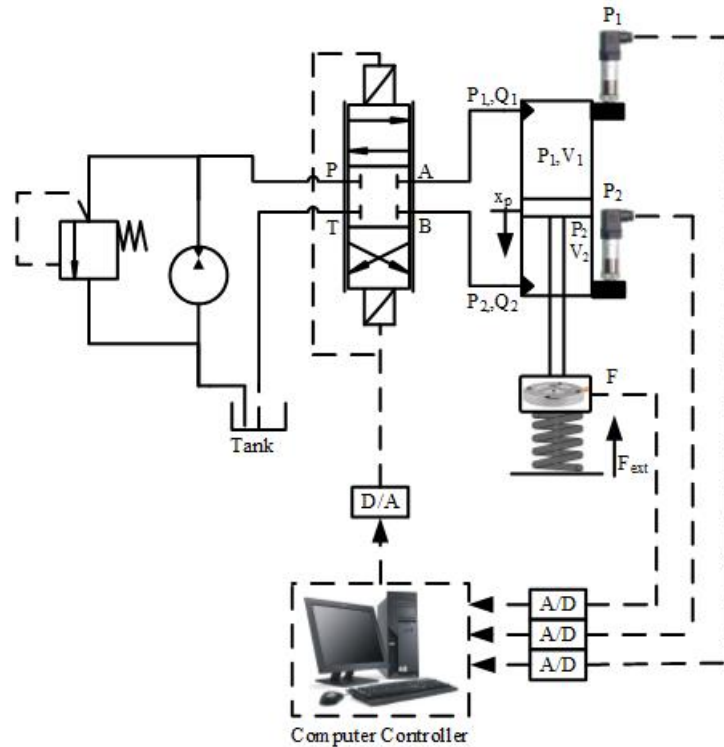


FIGURE 1. Schematic diagram of EHS

Equations (2) and (3) present the pressure changes in the cylinder for the compressible flow.

$$\dot{P}_1 = \frac{\beta}{V_{01} + A_1x_p}(Q_1 - A_1\dot{x}_p) \tag{2}$$

$$\dot{P}_2 = \frac{\beta}{V_{02} + A_2x_p}(A_2\dot{x}_p - Q_2) \tag{3}$$

The piston motion is controlled by the flow through a proportional valve. The voltage command to the proportional valve is related to the flow rates of high pressure fluid flow.

The oil flow rate is assumed to be in a linear relationship with the valve command signal (V_{in}), and flow rates Q_1 and Q_2 are shown in Equations (4) and (5) respectively. γ is the area ratio A_1/A_2 . The bandwidth of the control valve is around 100 Hz which is much faster than the dynamics of the cylinder actuator [21]. The valve dynamic is neglected.

$$Q_1 = \begin{cases} K_v V_{in}, & \dot{x}_p > 0 \\ \gamma K_v V_{in}, & \dot{x}_p < 0 \end{cases} \tag{4}$$

$$Q_2 = \begin{cases} \frac{K_v V_{in}}{\gamma}, & \dot{x}_p > 0 \\ K_v V_{in}, & \dot{x}_p < 0 \end{cases} \quad (5)$$

Since a linear spring is connected to the end of the piston, the motion of the piston is described by definition (6).

$$x_p = \frac{F}{k_s}, \quad \dot{x}_p = \frac{\dot{F}}{k_s} \quad \text{and} \quad \ddot{x}_p = \frac{\ddot{F}}{k_s} \quad (6)$$

Substituting Equation (6) into (1) yields,

$$\ddot{F} = \frac{k_s}{m}(P_1 A_1 - P_2 A_2) - \frac{c}{m} \dot{F} - \frac{k_s}{m} F \quad (7)$$

Replacing Equation (7) into (2) and (3) yields,

$$\dot{P}_1 = \frac{\beta}{k_s V_{01} - A_1 \dot{F}} (k_s Q_1 - A_1 \dot{F}) \quad (8)$$

Therefore,

$$\dot{P}_2 = \frac{\beta}{k_s V_{02} - A_2 \dot{F}} (A_2 \dot{F} - k_s Q_2) \quad (9)$$

Figure 2 shows the definition of each state variable in an EHS and Equation (10) shows the states equation of the system.

$$\begin{aligned} x_1 &= F \\ x_2 &= dF/dt \\ x_3 &= P_1 A_1 - P_2 A_2 \end{aligned} \quad (10)$$

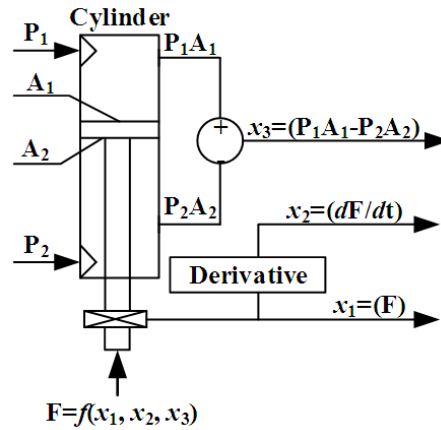


FIGURE 2. The definitions of state variables of an EHS

Rearrange Equations (7)-(9) to obtain the nonlinear model of an EHS strict-feedback form as,

$$\begin{aligned} \dot{x}_1 &= x_2 \\ \dot{x}_2 &= -\psi_2 x_1 - \psi_1 x_2 + \psi_2 x_3 \\ \dot{x}_3 &= -\varphi_1(x_1)x_2 + \varphi_2(x_1)u \end{aligned} \quad (11)$$

where,

$$\psi_1 = \frac{c}{m}, \quad \text{and} \quad \psi_2 = \frac{k_s}{m}$$

$$\begin{aligned}\varphi_1(x_1) &= \frac{\beta A_1^2}{k_s V_{01} + A_1 x_1} + \frac{\beta A_2^2}{k_s V_{02} - A_2 x_1} \\ \varphi_2(x_1) &= \frac{\beta A_1^2 K_v k_s}{k_s V_{01} + A_1 x_1} + \frac{\beta A_2^2 K_v k_s}{(k_s V_{02} - A_2 x_1)\gamma} \\ \text{and } u &= \begin{cases} V_{in}; & \dot{x}_p > 0 \\ \gamma V_{in}; & \dot{x}_p < 0 \end{cases}\end{aligned}$$

3. Controller Design. The backstepping method is a Lyapunov-based design technique which can be applied directly to strict-feedback nonlinear systems. The process starts with defining error for each state as,

$$e_i = x_i - x_{id}$$

where $i = 1, 2, 3$ are the error index for each state, x_{1d} is reference signal, x_{2d} and x_{3d} are visual control signals of each state. The process of control law design is presented in this section as follows.

Step 1: The system tracking error in first state can be defined as,

$$e_1 = x_1 - x_{1d} = x_1 - r$$

Then, the time derivative term of the tracking error is,

$$\dot{e}_1 = \dot{x}_1 - \dot{r} = x_2 - \dot{r}$$

The positive definition of Lyapunov function, $V_1(x_1)$, is,

$$V_1(x_1) = \frac{1}{2}e_1^2$$

Then, the time derivative of Lyapunov function is,

$$\dot{V}_1(x_1) = e_1 \dot{e}_1 = e_1(x_2 - \dot{r})$$

Define the virtual control signal (x_{2d}) so that the first time derivative of Lyapunov function V_1 is negative,

$$x_2 = x_{2d} = \dot{r} - k_1 e_1, \quad k_1 > 0$$

Thus,

$$\dot{V}_1(x_1) = -k_1 e_1^2 < 0$$

Step 2: Let the tracking error of the second state be,

$$e_2 = x_2 - x_{2d}$$

Then, the first time derivative of tracking error, e_2 , is

$$\dot{e}_2 = \dot{x}_2 - \dot{x}_{2d} = (-\psi_2 x_1 - \psi_1 x_2 + \psi_2 x_3) - \dot{x}_{2d}$$

Again, consider a Lyapunov function, $V_2(x_1, x_2)$,

$$V_2(x_1, x_2) = V_1(x_1) + \frac{1}{2}e_2^2$$

Then, the first time derivative of Lyapunov function V_2 is,

$$\dot{V}_2(x_1, x_2) = -k_1 e_1^2 + e_2 \dot{e}_2 = -k_1 e_1^2 + e_2(-\psi_2 x_1 - \psi_1 x_2 + \psi_2 x_3 - \dot{x}_{2d})$$

Define the virtual control signal (x_{3d}) so that the first time derivative of Lyapunov function V_2 is negative,

$$x_3 = x_{3d} = \frac{1}{\psi_2}(\psi_2 x_1 + \psi_1 x_2 + \dot{x}_{2d} - k_2 e_2)$$

where, $k_2 > 0$ and $\psi_2 \neq 0$. Thus,

$$\dot{V}_2(x_1, x_2) = -k_1 e_1^2 - k_2 e_2^2 < 0$$

Step 3: Let the system tracking error in last state can be defined as,

$$e_3 = x_3 - x_{3d}$$

Then, the time derivative term of tracking error is calculated as,

$$\dot{e}_3 = \dot{x}_3 - \dot{x}_{3d} = -\varphi_1(x_1)x_2 + \varphi_2(x_1)u - \dot{x}_{3d}$$

Again, consider a Lyapunov function.

$$V_3(x_1, x_2, x_3) = V_2(x_1, x_2) + \frac{1}{2}e_3^2$$

Then, the time derivative of Lyapunov function V_3 is

$$\dot{V}_3(x_1, x_2, x_3) = -k_1e_1^2 - k_2e_2^2 + e_3\dot{e}_3 = -k_1e_1^2 - k_2e_2^2 + e_3(-\varphi_1(x_1)x_2 + \varphi_2(x_1)u - \dot{x}_{3d})$$

The real control signal (u) is,

$$u = \frac{1}{\varphi_2(x_1)}(\varphi_1(x_1)x_2 + \dot{x}_{3d} - k_3e_3) \quad (12)$$

where, $k_3 > 0$ and $\varphi_2(x_1) \neq 0$. Thus,

$$\dot{V}_3(x_1, x_2, x_3) = -k_1e_1^2 - k_2e_2^2 - k_3e_3^2 < 0$$

Equation (12) is the control law of backstepping controller. The signal u is the command signal for controlled force x_1 to track a reference signal. The gains controller k_1 , k_2 and k_3 are optimized by using PSO algorithm.

3.1. States observer design. The backstepping control algorithm used in this study needs the information of 3 states. Two approaches are studied and compared. The values of all states are measured and calculated for the first approach. For the second approach, only x_1 is measured, and the values of two other states are estimated by a linear reduced order observer.

$$\mathbf{A} = \begin{bmatrix} 0 & 1 & 0 \\ -\psi_2 & -\psi_1 & \psi_2 \\ 0 & -\frac{\beta A_1^2}{k_s V_{01}} - \frac{\beta A_2^2}{k_s V_{02}} & 0 \end{bmatrix}, \mathbf{B} = \begin{bmatrix} 0 \\ 0 \\ -\frac{\beta A_1 K v}{V_{01}} - \frac{\beta A_2 K v}{V_{02} \gamma} \end{bmatrix}, \mathbf{C} = [1 \ 0 \ 0] \quad (13)$$

The EHS mathematical model (11) is linearized based on the Taylor series expansion. The $\varphi_1(x_1)$ and $\varphi_2(x_1)$ parameters in Equation (11) are linearized. To case the linearization, define the following: $k_s V_{01} + A_1 x_1 \approx k_s V_{01}$, $k_s V_{02} + A_1 x_1 \approx k_s V_{02}$ and $(k_s V_{02} + A_2 x_1) \gamma \approx k_s V_{02} \gamma$.

The linearization was performed around an operating point at $x_1 = 1000\text{N}$, $x_2 = 0\text{N/s}$ and $x_3 = 1000\text{N}$. Matrices \mathbf{A} , \mathbf{B} and \mathbf{C} of the linearized mathematical model are shown in Equation (13). Then, substituting all parameters in Table 1. Finally, the constant matrices of the mathematical model are shown in Equation (14). Note that all parameters in Table 1 are real specifications of each part in EHS.

$$\mathbf{A} = \begin{bmatrix} 0 & 1 & 0 \\ -2 \times 10^8 & -6 \times 10^3 & 2 \times 10^8 \\ 0 & -1.011 \times 10^7 & 0 \end{bmatrix}, \mathbf{B} = \begin{bmatrix} 0 \\ 0 \\ 3.1124 \times 10^6 \end{bmatrix}, \mathbf{C} = [1 \ 0 \ 0] \quad (14)$$

Figure 3 shows the scheme for the observer state estimate. The observer design is started from Equation (15).

$$\dot{\hat{x}} = A\hat{x} + Bu + K(y - C\hat{x}) \quad (15)$$

where, K is observer gain matrix. u is control signal. y is process measurement.

TABLE 1. Parameters setup of EHS

Symbol	Parameters	Value
β	Effective bulk modulus	$1.5 \times 10^9 \text{N/m}^2$
c	Viscous damping coefficient	500N/m.s^{-1}
A_1	Piston area side head-end	$1.256 \times 10^{-3} \text{m}^2$
A_2	Piston area side rod-end	$6.408 \times 10^{-4} \text{m}^2$
V_{01}	Initial head-end volume at $x_p = 0$	$3.141 \times 10^{-5} \text{m}^3$
V_{02}	Initial rod-end volume at $x_p = 0$	$1.602 \times 10^{-5} \text{m}^3$
m	Mass of piston	5kg
K_v	Flow/signal gain of valve	$3.7 \times 10^{-6} \text{m}^3/\text{V}$
k_s	Stiffness spring	$2 \times 10^5 \text{N/m}^2$

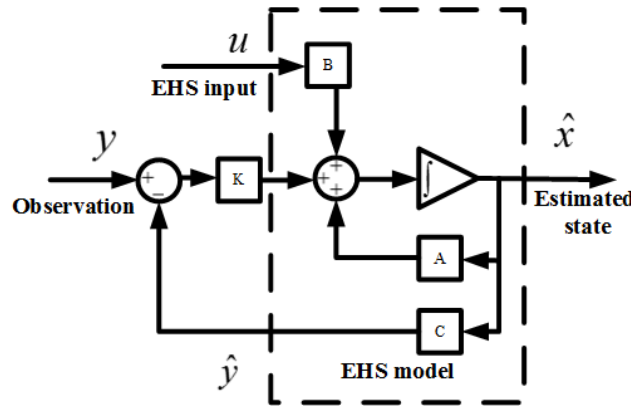


FIGURE 3. Observer states estimate scheme

The calculation of matrix K can be done in various ways such as optimization and pole-placement method. The kalman filtering algorithm is used for calculating matrix K in this study.

$$K = PC^T R^{-1} \tag{16}$$

P is the covariance matrix of the estimation error and satisfies the matrix of Riccati Equation (17).

$$AP + PA^T - PC^T R^{-1} CP + Q = 0 \tag{17}$$

R is a positive-definite matrix and Q is a positive or semi-definite matrix. The matrices R and Q are measured between control signal and output force signal that are approximately equal to 0.01V and 10N, respectively. Thus, the observation and process noise covariance are $Q = 0.01^2(BB^T)$ and $R = 10^2$. Note that matrix Q is to be used as state estimates in the close-loop control system. The LQE command in MATLAB function is used to solve the Algebraic Riccati Equation, and obtain the matrix K .

$$K = [0.0589 \quad 0.173 \quad -0.395] \tag{18}$$

3.2. PSO-backstepping design. The PSO was introduced by Eberhart and Kennedy in 1995. This method is a stochastic algorithm based on the principles of natural selection. The controller gains are equivalent to the particles in PSO algorithm. The controller gains are tuned for three step inputs (k_1 , k_2 and k_3) following the control law described in Equation (12). Particles of positions x_i are related to controller gains k_1 , k_2 and k_3 with its corresponding velocities v_i . The velocity of each particle is updated in the next step (according to Equation (19)). The position of each particle is then updated in the final

step according to Equation (20).

$$v_i = w \cdot v_{i-1} + c_1 \cdot R_1 \cdot (P_{best} - x_{i-1}) + c_2 \cdot R_2 \cdot (G_{best} - x_{i-1}) \quad (19)$$

$$x_i = x_{i-1} + v_i, \quad i = 1, 2, \dots, n \quad (20)$$

where, n is the number of particles in the group. R_1 and R_2 are random numbers between 0 to 1. c_1 and c_2 are acceleration constants, v_{i-1} is the velocity of the previous particle movement, x_{i-1} is the previous position, P_{best} is the best value of all individual and G_{best} is global best position. The initial values of the parameters used in Equations (19) and (20) are shown in Table 2. More information on the definition of the PSO can be found in [22,23].

TABLE 2. The initial parameters of PSO

PSO Property	Value
Population number	5
Maximum iteration	250
Social coefficient (c_1)	2.0
Cognitive coefficient (c_2)	2.0
Performance index	<i>ITAE</i>
Inertial weight (w)	0.8
Lower limit of [k_1 k_2 k_3]	[0 0 0]
Upper limit of [k_1 k_2 k_3]	[15000 500 100]

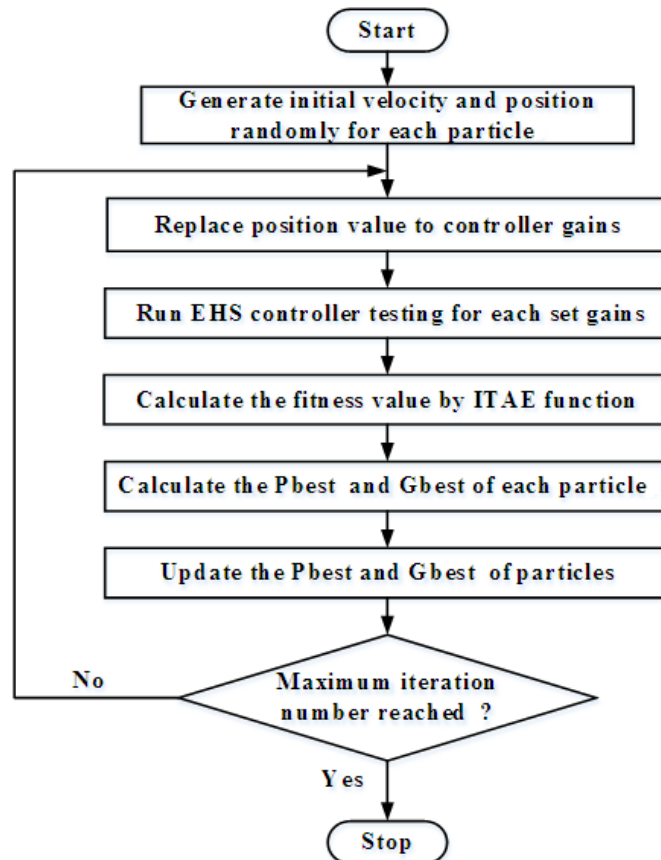


FIGURE 4. The PSO algorithm process

3.3. The process of tuning a PSO-backstepping. Figure 4 shows the sequence of the gain tuning process and can be explained as follows.

(i) The backstepping controller needs three gains controller $[k_1 \ k_2 \ k_3]$. The population number was chosen to be five sets. Therefore, the dimensions of the position and velocity matrices are both 3×5 . These two matrices are generated randomly, such as the values of all elements within the lower and upper bounds. Both matrices are the initial particles of positions x_i and velocities v_i .

(ii) Each row of the position matrix contains the controller gains $[k_1 \ k_2 \ k_3]$ of each population set: the first row belongs to the first set, the second row belongs to the second set and so on. All sets of position (or controller gains) are tested experimentally in the EHS. The fitness value for each set of position particles is then obtained according to the integral of time multiplied by absolute error (ITAE) function in Equation (21).

$$ITAE = \int_0^{\infty} t |e(t)| dt \quad (21)$$

(iii) The P_{best} is chosen by comparing fitness value in each cycle. The set of the position particles that give the minimum fitness value is set to be the P_{best} of this cycle. G_{best} is then obtained by comparing the current P_{best} with all previous values of P_{best} .

(iv) The velocity and position in the next cycle are updated by Equations (19) and (20) using the values of P_{best} and G_{best} from step (iii).

(v) The whole process is repeated until the condition defined previously is satisfied. In this study the process is run for 250 cycles.

4. Experimental Results. The optimal gains of backstepping controller with observed states and measured states were obtained experimentally using the PSO algorithm. A 1000N force step command is used in the PSO training, where 250 cycles were implemented for each training case. With 9 seconds per cycle, it took 37.5 minutes to obtain the optimal gains. The process of finding optimal gains follows that shown in Figure 4 and the ITAE function in Equation (21) was used to indicate the optimal gain.

Figure 5 shows the fitness values of the backstepping controller using observed states and measured states. Both fitness values are optimized by PSO algorithm. This method can increase value from 4000 to the best value within 250 cycle times. The optimal fitness

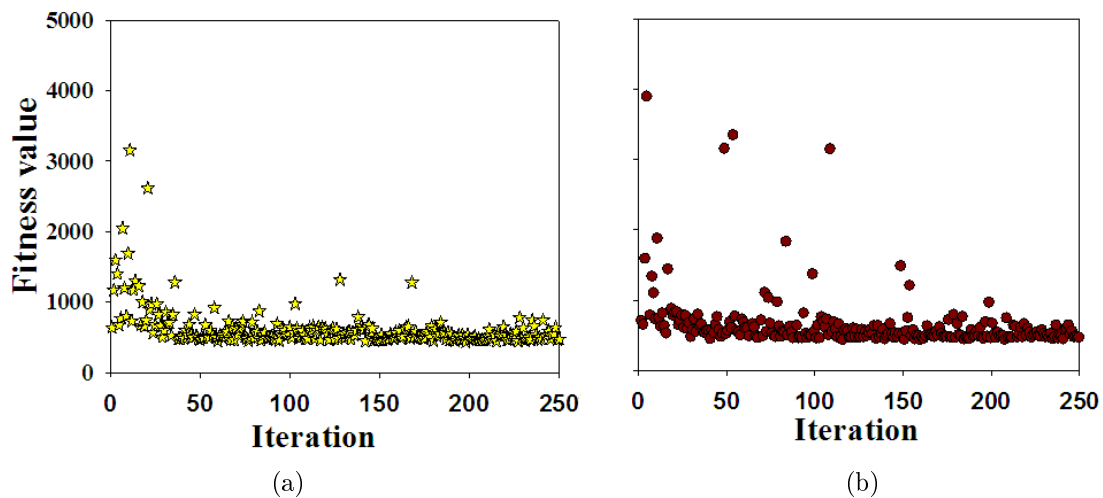


FIGURE 5. Fitness value of step input of (a) controller using real states and (b) controller using estimated states

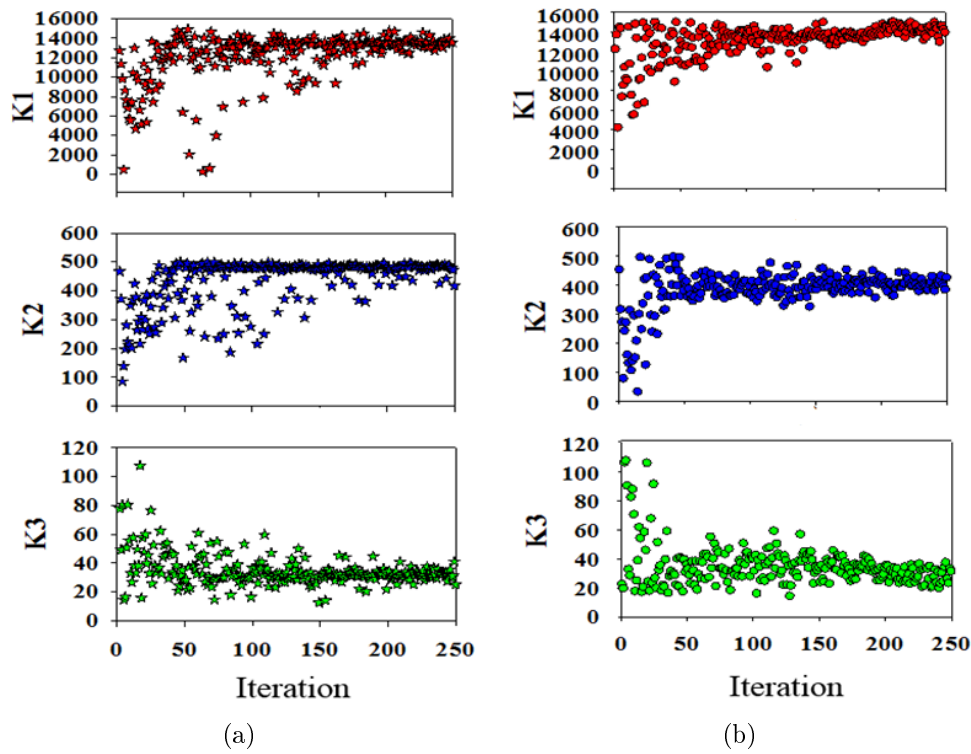


FIGURE 6. The convergence of controller gains of (a) controller using real states and (b) controller using estimated states

TABLE 3. Optimal gains of PSO based on backstepping

Controllers	Fitness value	Optimal gains
PSO-based backstepping in real states	427.76	$k_1 = 13550.7$
		$k_2 = 483.54$
		$k_3 = 32.03$
PSO-based backstepping in estimated states	433.17	$k_1 = 14510.07$
		$k_2 = 401.77$
		$k_3 = 27.49$

values were found to be 433.17 and 427.76 for the observed states and measured states, respectively. Figure 6 shows the convergence of controller gains for both controllers, which resembles the convergence of the fitness values. The optimal gains k_1 , k_2 and k_3 were found within 50 cycles after which the tuning was more refined. The best backstepping controller's gains were found for both observed state and measured state cases.

Table 3 shows the values of the optimal controller gains of both controllers.

Figure 7 shows the response of using the best gains $[k_1 \ k_2 \ k_3]$. It can be observed that the rise time of 0.4 seconds was achieved with no overshooting. The responses in both cases were not different, indicating the capability of the state estimation. Figure 8 shows the convergence of the observed state compared with the measured values. The measured state x_3 (Equation (10)) shows approximately 360 Vpp noise due to the noise picked up at the pressure transducers. Though the observed state signal was different from the measured one, the step response of EHS still shows effective force tracking. Figure 9 shows the comparison results of a force square input. The bound amplitude of square signal is 1000N and 200N at 1Hz of frequency. The controller gains from Table 3 are used

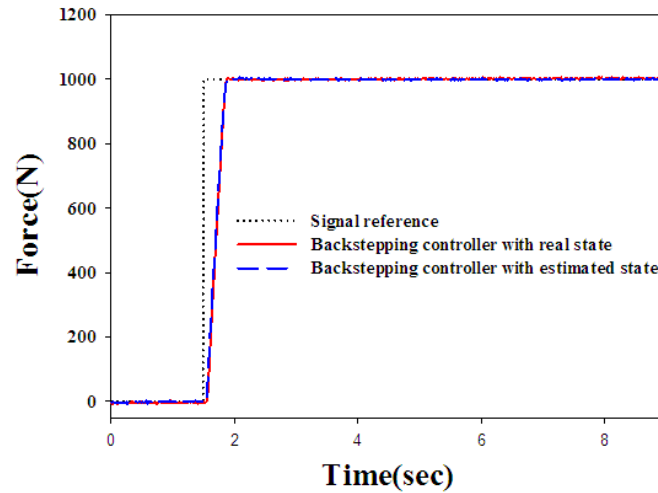


FIGURE 7. Step response

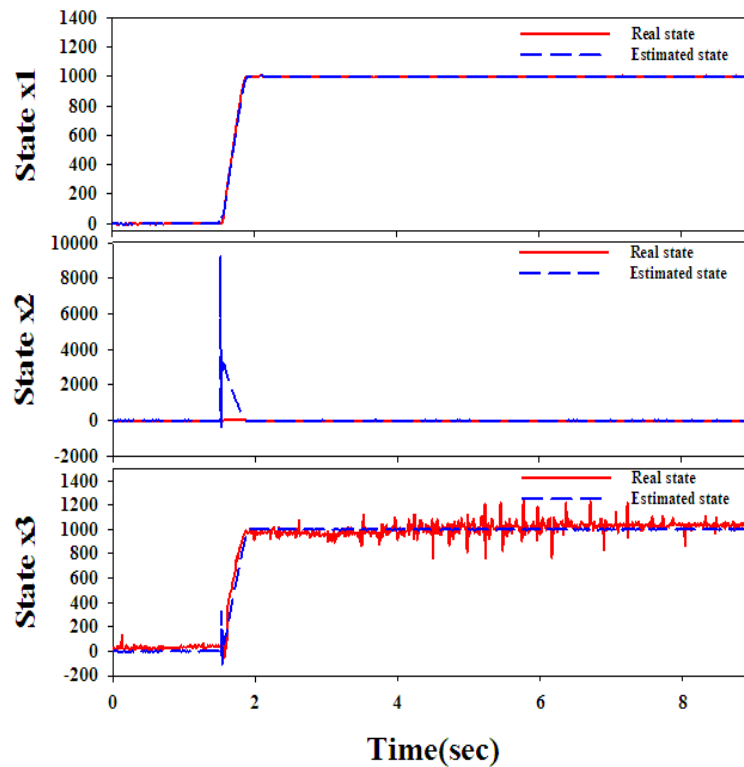


FIGURE 8. States comparison

in this experiment. Both controllers yield almost identical tracking performance, both exhibiting the rise time of 0.35 seconds. No significant overshooting was observed.

Figure 10 shows the convergence of the value of each observed state comparing with the measured values in the square input. The measured state x_3 shows a small degree of noise (360 Vpp), resembling the states comparison in the step input.

5. Conclusions. A backstepping controller was implemented on a force-controlled electro-hydraulic system. The backstepping controller gains were optimally obtained by using the PSO technique. Two types of controller were designed and tested: backstepping with observed states and backstepping with measured states. Both controllers were tested and

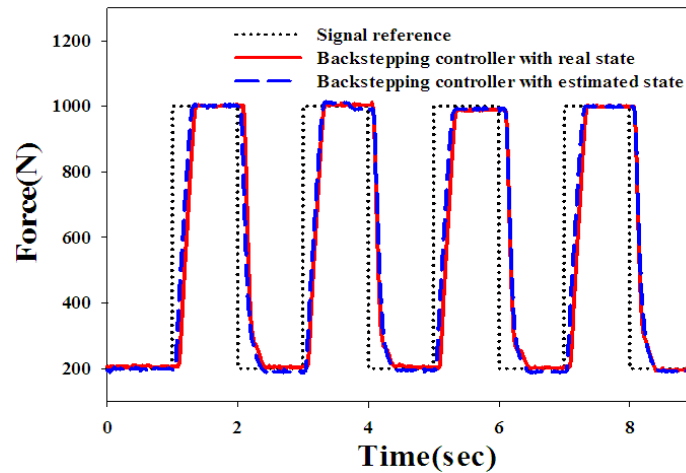


FIGURE 9. Square response

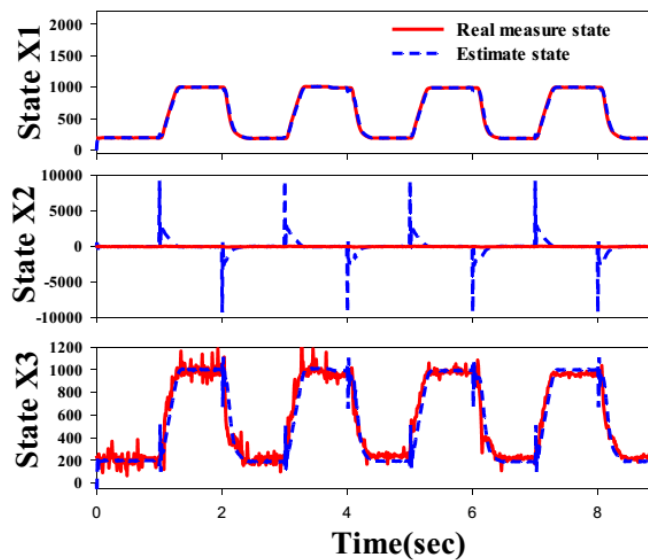


FIGURE 10. States comparison

compared by using a square wave input. The experimental results show the effectiveness of the force tracking and the searching for controller gains. The PSO algorithm was proven to be an effective tool for finding the optimal gains for the backstepping controller with both observed and measured states. The backstepping controller when implemented with observed states could save the cost of measuring devices without sacrificing the tracking performance.

REFERENCES

- [1] N. D. Manring, *Hydraulic Control Systems*, John Wiley & Sons, Hoboken, 2005.
- [2] A. R. Plummer and A. D. Vaughan, Decoupling pole-placement control with application to a multi-channel electro-hydraulic servo system, *Control Eng. Pract.*, 1997.
- [3] J. Seo, R. Venugopal and J. Kenné, Feedback linearization based control of a rotational hydraulic drive, *Control Eng. Pract.*, vol.15, pp.1495-1507, 2007.
- [4] Q. H. Nguyen, Q. P. Ha, D. C. Rye and H. F. Durrant-Whyte, Feedback linearisation control for electro-hydraulic systems of a robotic excavator, *Proc. of Australian Conference on Robotics and Automation*, Brisbane, pp.190-195, 1999.

- [5] A. Alleyne and R. Liu, A simplified approach to force control for electro-hydraulic systems, *Control Eng. Pract.*, 2000.
- [6] S. Alshamali and M. Zribi, Backstepping control design for a continuous-stirred tank, *International Journal of Innovative Computing, Information and Control*, vol.8, no.11, pp.7747-7760, 2012.
- [7] M. Ahmadnedzhad and M. Soltanpour, Tracking performance evaluation of robust back-stepping control design for a nonlinear electrohydraulic servo system, *International Journal of Mechanical, Aerospace, Industrial, Mechatronic and Manufacturing Engineering*, vol.9, no.7, 2015.
- [8] M. R. Sirouspour and S. E. Salcudean, On the nonlinear control of hydraulic servo-systems, *Proc. of the 2000 IEEE International Conference on Robotics & Automation*, San Francisco, CA, 2000.
- [9] A. Mohanty and B. Yao, Indirect adaptive robust control of hydraulic manipulators with accurate parameter estimates, *IEEE Trans. Control Syst. Technol.*, vol.19, no.3, 2011.
- [10] B. Yao, F. Bu and G. T. C. Chiu, Non-linear adaptive robust control of electro-hydraulic systems driven by double-rod actuators, *Int. J. Control*, vol.74, no.8, pp.761-775, 2001.
- [11] J. Ye, Tracking control for nonholonomic mobile robots: Integrating the analog neural network into the backstepping technique, *Neurocomputing*, vol.71, nos.16-18, pp.3373-3378, 2008.
- [12] C. K. Chen, W. Y. Wang, Y. G. Leu and C. Y. Chen, Compact ant colony optimization algorithm based fuzzy neural network backstepping controller for MIMO nonlinear systems, *Proc. of the International Conference on System Science and Engineering*, Taipei, Taiwan, pp.146-149, 2010.
- [13] R. Eberhart and I. Kennedy, A new optimizer using particle swarm theory, *Proc. of the 6th Int. Symposium on Micro Machine and Human Science*, pp.39-43, 1995.
- [14] J. Kennedy and R. C. Eberhart, Particle swarm optimization, *Proc. of the IEEE International Conference on Neural Networks IV*, pp.1942-1948, 1995.
- [15] M. H. Ibrahim and A. R. Osama, Particle swarm optimization approach for solving complex variable fractional programming problems, *Journal of Engineering Research & Technology*, vol.2, 2013.
- [16] A. Ahmed, A. Esmin and G. Lambert-Torres, Application of particle swarm optimization to optimal power systems, *International Journal of Innovative Computing, Information and Control*, vol.8, no.3(A), pp.1705-1716, 2012.
- [17] S. M. Roazli, M. F. Rahmat and A. R. Husain, Performance comparison of particle swarm optimization and gravitational search algorithm to the designed of controller for nonlinear system, *Journal of Applied Mathematics*, 2014.
- [18] S. Panda and N. P. Padhy, Comparison of particle swarm optimization and genetic algorithm for FACTS-based controller design, *Applied Soft Computing*, pp.1418-1427, 2008.
- [19] H. Xing, X. Zhong and J. Li, Linear extended state observer based back-stepping control for uncertain SISO nonlinear systems, *International Journal of Innovative Computing, Information and Control*, vol.11, no.4, pp.1411-1419, 2015.
- [20] H. E. Merrit, *Hydraulic Control System*, Wiley & Sons, New York, 1967.
- [21] Robert Bosch GmbH, *Electro-Hydraulic Proportional and Control System*, Omegon, Ditzingen, 1999.
- [22] R. F. Stengel, *Optimal Control and Estimation*, Dover Publications, New York, 1994.
- [23] S. Ebbesen, P. Kiwitez and L. Guzzella, A generic particle swarm optimization Matlab function, *American Control Conference*, Fairmont Queen Elizabeth, Montreal, Canada, 2012.